JOURNAL OF VIROLOGY, Aug. 1995, p. 5011–5017 Vol. 69, No. 8
0022-538X/95/$04.00+0

Steps in Maturation of Influenza A Virus Neuraminidase

TAKEHIKO SAITO,[1,2] GARRY TAYLOR,[3] AND ROBERT G. WEBSTER[1,4]*

Department of Virology/Molecular Biology, St. Jude Children's Research Hospital, Memphis, Tennessee 38101[1]; Department of Animal Science, Faculty of Agriculture, Kobe University, Kobe 657, Japan[2]; Department of Biochemistry, University of Bath, Claverton Down, Bath BA2 7AY, United Kingdom[3]; and Department of Pathology, University of Tennessee, Memphis, Memphis, Tennessee 38163[4]

Received 19 December 1994/Accepted 21 April 1995

We have studied the maturation of the influenza A virus neuraminidase (NA), using monoclonal antibodies (MAbs) with different conformational specificities against the head domains of the N8 NA. The results obtained with radioimmunoprecipitation, together with previously published information, suggest the following steps in maturation of this molecule. First, the folding of the nascent NA leads to formation of the epitope recognized by MAb N8-10, a step that depends on the formation of intramolecular disulfide bonds. Second, monomers form dimers by an intermolecular disulfide linkage in the stalk, with a $t_{1/2}$ of 2.5 min. Third, the epitope recognized by MAb N8-82 appears after dimerization, suggesting that oligomeric NAs may undergo conformational change with a $t_{1/2}$ of 8 min. Finally, a tetramer-specific epitope recognized by MAb N8-4 appears on the NA with a $t_{1/2}$ of 13 min. Epitope detection by MAb N8-4 was inhibited by tunicamycin treatment, suggesting that glycosylation of this molecule is required for proper tetramerization. Each of these proposed steps occurs in the endoplasmic reticulum of host cells, as demonstrated by treatment of virus-infected cells with brefeldin A or carbonyl cyanide *m*-chlorophenylhydrazine; subsequently, tetrameric NA is transported to the Golgi apparatus, where oligosaccharide processing is completed. Our findings also provide a possible explanation—lack of a functionally active conformation—for the absence of enzymatic function by NA monomers.

Viral membrane proteins undergo sequential steps in their maturation, including the folding and assembly of subunits before their integration into virions (for review, see reference 11). Influenza A virus has two membrane glycoproteins, hemagglutinin (HA) and neuraminidase (NA). The HA is a type I protein whose folding and assembly have been studied in detail (9, 15, 24, 26). The nascent molecule is folded during and after translation and is assembled into trimers on completion of folding. Trimerization appears to be a prerequisite for HA transport from the endoplasmic reticulum (ER) of the host cell. The NA, a type II glycoprotein on the surface of the viral envelope, is a tetramer with three distinct domains: a globular head containing the enzyme active site and most of the antigenic sites, a stalk region containing a hydrophobic region by which this enzyme is embedded in the viral envelope, and a cytoplasmic tail (1). Despite extensive study of the three-dimensional structures of the head domains of the NA (8, 25), little is known about the maturation of this integral membrane protein (16).

Monoclonal (MAbs) and polyclonal antibodies are useful tools for exploring the process of protein maturation (10). Some antibodies are specific for a particular maturational stage or oligomeric form of a protein. A panel of MAbs against the head domain of the N8 NA derived from strain A/duck/Ukraine/1/63 has been established (21). The neuraminidase-inhibiting MAbs are divided into three groups (I, II, and III) based on their reactivities with escape mutants. MAb N8-10 (group I) immunoprecipitates the monomeric, dimeric, and tetrameric forms of the NA, while N8-4 (group II) binds specifically to the tetramer (21). A third MAb, N8-82 (group III), characterized in this report, recognizes an epitope formed after dimerization. By exploiting the different conformational specificities of these antibodies against metabolically labeled NAs, we have identified discrete molecular steps in the maturation of this viral envelope glycoprotein.

* Corresponding author. Mailing address: Department of Virology/Molecular Biology, St. Jude Children's Research Hospital, Memphis, TN 38101. Phone: (901) 495-3400. Fax: (901) 523-2622.

MATERIALS AND METHODS

Cells and virus. Madin-Darby canine kidney (MDCK) cells were maintained in minimal essential medium (MEM) with 5% fetal calf serum. The reassortant influenza virus NWS-Dk/Ukraine (H1N8; NWS-N8), which possesses the HA gene from A/NWS/33 and the NA gene from A/duck/Ukraine/1/63 (25), was used exclusively in these studies. The numbering of amino acid residues in the N8 head follows the conventional N2 numbering system.

Metabolic labeling and immunoprecipitation of NA. Confluent monolayers of MDCK cells in 25-cm^2 culture flasks were infected with 10^9 50% egg infectious doses (EID_{50}) of NWS-N8 in MEM with 0.3% bovine serum albumin (MEM-BSA) and incubated for 1 h at 37°C. After addition of 4 ml of MEM-BSA, incubation was continued for another 4 h at 37°C in 5% CO_2. The cells were then washed with warmed phosphate-buffered saline (PBS) twice, and 1 ml of methionine-free MEM was added for 15 min. For experiments designed to examine the role of glycosylation, tunicamycin (TM) was added at 3 h postinfection to a final concentration of 1 μg/ml, which was maintained throughout the procedure described below.

Two hundred microcuries of [^{35}S]methionine (Trans^{35}S; ICN, Irvine, Calif.) was added to the medium for pulse labeling, after which the cells were washed with warm PBS twice, and the medium was replaced with MEM containing 10 times the concentration of unlabeled methionine for chase. To examine the effect of low temperature on NA maturation, we adjusted the chase medium to 15°C and performed incubations in a 15°C water bath. ATP was depleted by adding carbonyl cyanide *m*-chlorophenylhydrazine (CCCP) to the chase medium. At the end of the chase period, cells were washed with cold PBS twice, harvested, and lysed in 50 mM Tris (pH 7.5)–100 mM NaCl–1% Triton X-100–20 mM iodoacetamide for 30 min on ice. After removal of cell debris by microcentrifugation, cell lysates were incubated overnight with MAb at 4°C. Antigen-antibody complexes were precipitated by rabbit anti-mouse immunoglobulin (heavy- and light-chain specific) bound to beads (Immunobead Reagent; Bio-Rad, Hercules, Calif.). Samples were analyzed by sodium dodecyl sulfate–10% polyacrylamide gel electrophoresis (SDS-PAGE) under nonreducing conditions after boiling for 4 min (unless otherwise mentioned). Fluorographs were scanned with a Bio Image Visage 110 (Millipore, Ann Arbor, Mich.).

BFA treatment. Brefeldin A (BFA; Epicentre Technologies, Madison, Wis.) was added to the medium at 3 μg/ml 2 h before the labeling of virus-infected cells with [^{35}S]methionine. This concentration was maintained during the methionine depletion, labeling, and chase periods.

Gradient centrifugation. Virus-infected cells in 25-cm^2 culture flasks were pulse-labeled with 1 mCi of [^{35}S]methionine and chased with an excess of unla-

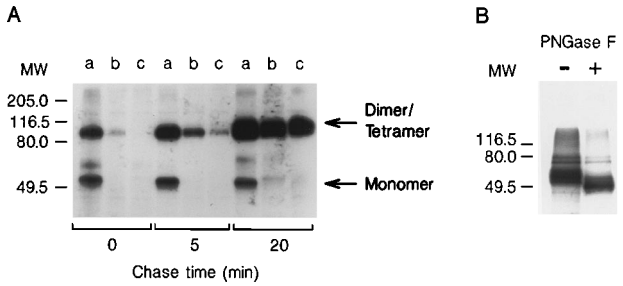

FIG. 1. Radioimmunoprecipitation of the N8 NA with MAbs. (A) Virus-infected cells were labeled with [^{35}S]methionine for 5 min and chased with unlabeled methionine as indicated. Lane a, MAb N8-10; lane b, MAb N8-82; lane c, MAb N8-4. (B) Cell lysates treated (+) or not (−) with PNGase F were immunoprecipitated with MAb N8-82. Samples were analyzed by SDS–14% PAGE under reducing conditions. Sizes are shown in kilodaltons.

beled methionine in the presence or absence of 1 mM CCCP. Cells were lysed in the Triton buffer described above, and after microcentrifugation, cell lysates were loaded onto a 5 to 25% sucrose gradient containing 0.1% Triton X-100 in the same buffer. Gradients were centrifuged for 16.5 h at 174,500 × *g* at 20°C in an SW41 rotor (Beckman). Thirty 400-μl fractions were collected from each tube and divided into two equal parts; the even-numbered fractions, 1 to 30 from the top to bottom of the tube, were immunoprecipitated with MAbs. Immunoprecipitates were analyzed by SDS–10% PAGE under nonreducing conditions. BSA (4.9S), aldolase (8.6S), and catalase (11.3S) were used as molecular markers.

Endo H treatment. Immunoprecipitations after [^{35}S]methionine labeling and chase were performed as described above. Immunoprecipitates were suspended in 130 μl of 100 mM sodium phosphate buffer (pH 5.9)–0.1% Triton X-100–0.02% SDS–20 mM EDTA. The suspensions were incubated for 3 min at 100°C and then divided into two equal parts. One was treated with 5 mU of endoglycosidase H (Endo H; Boehringer Mannheim, Indianapolis, Ind.) overnight at 37°C, while the other served as a control. After overnight incubation, each sample was analyzed by SDS–10% PAGE under reducing conditions.

PNGase F treatment. Virus-infected cells were labeled with [^{35}S]methionine for 30 min and then were lysed in 100 mM sodium phosphate buffer (pH 7.1)–20 mM EDTA–0.1% SDS–1% Triton X-100. After removal of cell debris by centrifugation, the lysates were divided into two equal parts, one of which was treated with 6 U of peptide-*n*-glycosidase F (PNGase F; Beohringer Mannheim) overnight at 37°C, while the other was used as a control. After overnight incubation, both samples were subjected to immunoprecipitation as described earlier in this section.

RESULTS

MAb N8-82 recognizes the epitope not present on monomeric NA. NA-inhibiting MAbs are classified as group I, II, or III, depending on their reactivity with escape mutants (21). MAb

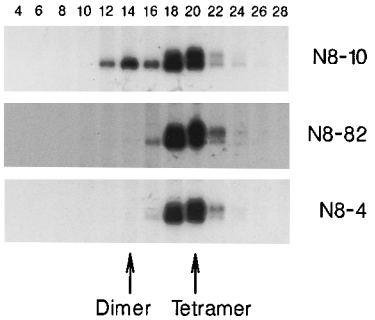

FIG. 2. Fractionation of radiolabeled cell lysates followed by immunoprecipitation with MAb N8-10 (upper panel), N8-82 (middle panel), or N8-4 (lower panel). Virus-infected cells were labeled with [^{35}S]methionine for 20 min, lysed, and subjected to sucrose gradient centrifugation. Immunoprecipitates were analyzed by nonreducing SDS-PAGE. The photographic print of MAb N8-82 was intentionally overexposed to show the trace amount of dimeric NA. BSA (4.9S), aldolase (8.6S), and catalase (11.3S) sedimented with peaks in fractions 6, 20, and 26, respectively, under identical conditions. Lane numbers are fraction numbers.

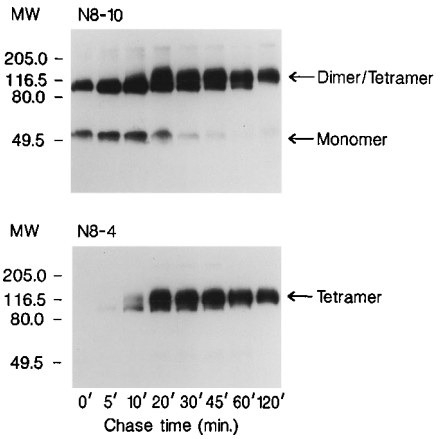

FIG. 3. Kinetics of dimerization and tetramerization of the N8 NA. Cells were labeled for 5 min and chased for up to 120 min, followed by immunoprecipitation with Mab N8-10 (upper panel) or N8-4 (lower panel). Sizes are shown in kilodaltons.

N8-82 recognizes an epitope involving amino acid residues 367, 399, and 400, for this group III antibody did not inhibit the enzyme activity of NA mutants with amino acid substitutions at residue 367 or 400, and its enzyme-inhibiting activity was greatly reduced on the mutant with a substitution at residue 399 (21). In the present study, MAb N8-82 precipitated dimeric NA at 0 min of chase (Fig. 1A), but failed to recognize monomeric NA.

Immediately after metabolic labeling of the NA for 5 min,

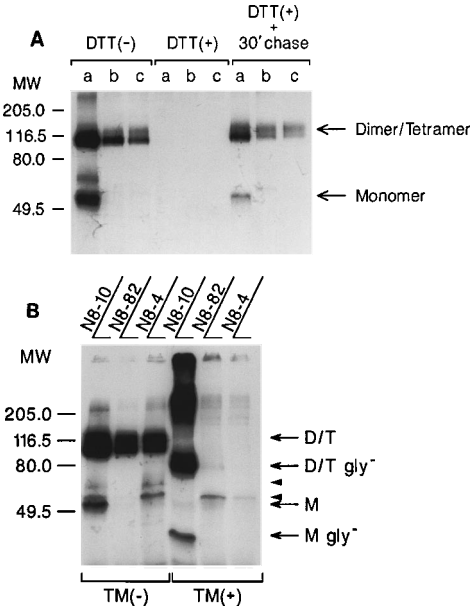

FIG. 4. Effect of DTT and TM on NA maturation. (A) Virus-infected cells were labeled with [^{35}S]methionine in the absence [DTT(−)] or presence [DTT(+)] of DTT for 20 min. Cells were lysed after labeling or further chased for 30 min without DTT [DTT(+) + 30-min chase], lysed, and immunoprecipitated with MAb N8-10 (lanes a), N8-82 (lanes b), or N8-4 (lanes c). (B) Virus-infected cells were treated with TM as described in Materials and Methods. Samples were immunoprecipitated with MAb N8-10, N8-82, or N8-4 as shown at the top of the panel. D/T, dimer and tetramer; M, monomer; D/T gly$^-$ and M gly$^-$, NAs without carbohydrate chains. The precipitates indicated by arrowheads are nonspecific, as these bands were not consistently detected in multiple experiments. Sizes are shown in kilodaltons.

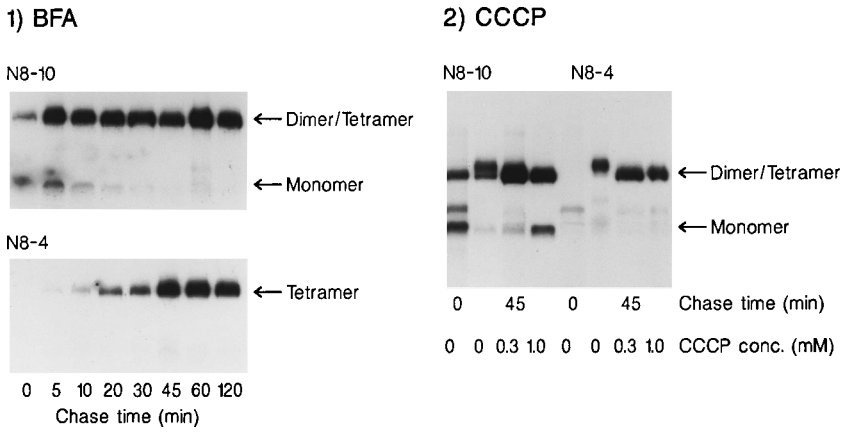

FIG. 5. Virus-infected cells were treated with either BFA or CCCP as described in Materials and Methods. BFA-treated cells were radiolabeled for 5 min and chased for up to 120 min. The cells were subjected to immunoprecipitation by MAb N8-10 (upper panel) or N8-4 (lower panel). For CCCP treatment, virus-infected cells were radiolabeled for 5 min and then chased with unlabeled methionine in the presence of various concentration of CCCP for either 0 or 45 min. Cells were subjected to immunoprecipitation as indicated.

marked differences in reactivity were apparent among MAbs N8-4, N8-10, and N8-82 on oligomeric NAs (Fig. 1A). MAb N8-10 immunoprecipitated both the monomer and the oligomer, whereas N8-4 did not precipitate either form. MAb N8-82 precipitated smaller amounts of the oligomeric NA and failed to precipitate the monomer altogether. At 5 min of chase, MAb N8-4 began to precipitate the NA tetramer, which dissociates into dimers upon electrophoresis (16, 21). At 20 min of chase, these three MAbs precipitated comparable amounts of NA (Fig. 1A), indicating that the previously noted differences in reactivity among these MAbs in fact reflect the kinetics of epitope formation. Carbohydrate side chains are not involved in epitope recognition by MAb N8-82, as demonstrated by the result of PNGase treatment (Fig. 1B), which cleaves all N-linked oligosaccharide moieties from glycoproteins. These results suggest that the NA oligomer may undergo conformational change during oligomeric maturation, leading to formation of the epitope recognized by MAb N8-82. The putative conformational change detected by this antibody occurs with a $t_{1/2}$ of 8 min, as demonstrated by an experiment similar to those shown in Fig. 1A.

To examine whether the epitope recognized by MAb N8-82 residues on the dimer or tetramer, we subjected virus-infected cell lysates to sucrose density centrifugation (Fig. 2). Oligomeric NAs with molecular masses of approximately 110 and 130 kDa were precipitated by MAb N8-10 in fractions 10 to 24. Two peaks of oligomeric NAs were observed in fractions 14 and 20. The former consisted of NAs with a molecular mass of 110 kDa and the latter of NAs of both 110 and 130 kDa. The tetramer-specific MAb N8-4 precipitated the latter peak exclusively. These results led us to designate fractions 14 and 20 as dimeric and tetrameric NAs, respectively; monomeric NA could not be detected because of its small quantity. MAb N8-82 precipitated tetrameric NA and a trace amount of NA in fractions 10 to 14, which might represent the dimeric form of the molecule. This observation suggests that the epitope recognized by MAb N8-82 may occur on dimeric NA, preceding tetramer formation. However, the small amount of NA in fractions 10 to 14 precludes any firm interpretation of the data.

Kinetics of folding of the NA. We also examined the kinetics of dimer and tetramer formation of the NA by radioimmunoprecipitation and taking advantage of the fact that MAb N8-4 recognizes only the tetrameric forms of the NA (21), while MAb N8-10 recognizes the epitope on the NA monomer. Precipitates obtained after each chase period were scanned and quantified. Maximum amounts of radiolabeled NA were precipitated by MAb N8-10 at 20 min of chase. On the other hand, at 0 min after labeling, only 47% of radiolabeled NA was precipitated by the same antibody compared with the results at 20 min of chase (Fig. 3). Thus, MAb N8-10 appears to recognize a conformation-dependent epitope of the NA, while the remainder of the NA is still not folded. Almost 70% of the NA precipitated with MAb N8-10 at this time was in the dimeric form. Although the observed dimeric NA was probably formed by intermolecular disulfide linkage at the stalk, we cannot rule out the possibility that a noncovalently linked dimer was formed before intermolecular disulfide linkage occurred and was dissociated into monomers by SDS-PAGE.

As judged from the appearance of the N8-4-reactive form, tetramerization had begun by 5 min of chase. The NA species of slower mobility on polyacrylamide gels appeared by 10 min of chase, indicating further processing of oligosaccharides. At 120 min of chase, most of the NA showed slower mobility on polyacrylamide gels, and the amount obtained by radioimmunoprecipitation with MAb N8-10 decreased to 40% compared with that obtained at 20 min of chase, results consistent with incorporation of the tetramer into virions, intracellular degradation, or both (16). The half-time of dimerization was approximately 2.5 min, while that of tetramer formation, estimated

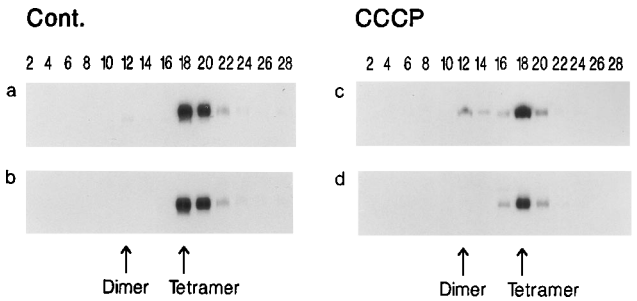

FIG. 6. Fractionation of CCCP-treated virus-infected cells. Virus-infected cells were radiolabeled for 5 min and then chased for 45 min in the presence (right panels) or absence (left panels, control) of 1 mM CCCP. Cell lysates were fractionated on 5 to 25% sucrose density gradients. Even-numbered fractions were immunoprecipitated with MAb N8-10 (a and c) or N8-4 (b and d).

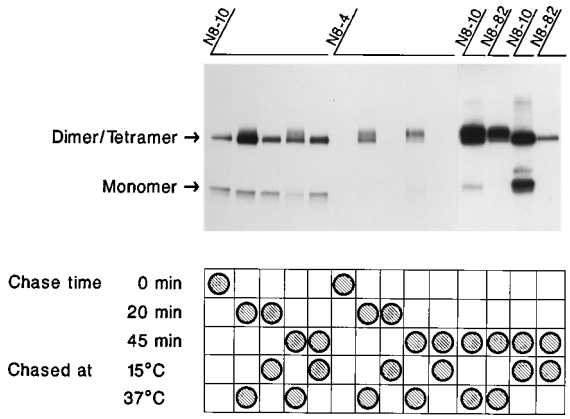

FIG. 7. Temperature sensitivity of NA maturation. The MAbs used for radioimmunoprecipitation are given at the top of the panel. After 5 min of labeling, the cells were chased for 0, 20, or 45 min, as indicated, at either 15 or 37°C.

from the appearance of N8-4 epitope, was approximately 13 min.

Implication of disulfide bonds and glycosylation during NA maturation. The formation of the epitope detected by MAbs N8-4, -10, and -82 depends on folding and assembly of the NA. Disulfide bond formation and glycosylation have been described as important factors for the proper folding and assembly of glycoproteins (11). To assess their involvement in NA epitope formation, we added dithiothreitol (DTT; 5 mM) to the medium during labeling with [^{35}S]methoinine to prevent disulfide bond formation in newly synthesized proteins (5, 24). After virus-infected cells were labeled for 20 min in the presence or absence of DTT, the cells were lysed and subjected to immunoprecipitation. The addition of DTT prevented the formation of the epitopes recognized by MAbs N8-4, -10, and -82 (Fig. 4A), indicating that disulfide linkage plays a crucial role in the folding of the NA and in epitope formation detected by these three MAbs. Further chase (30 min) with unlabeled methionine after removal of DTT and [^{35}S]methionine restored the normal maturation of the NA (Fig. 4A).

To determine the role of glycosylation in NA maturation, we inhibited this process with TM (1 μg/ml). None of the MAbs in our panel recognized carbohydrate chains as part of the epitope (Fig. 1B) (21). After TM treatment, the NAs precipitated by MAb N8-10 showed lower molecular masses than those observed without such treatment (Fig. 4B, D/T gly$^-$ versus D/T). In addition, a majority of the precipitates that probably represented aggregation of NAs that could not undergo proper assembly were found in a higher-molecular-mass portion of the gel. Sucrose gradient fractionation confirmed the presence of tetrameric NA and of aggregates with higher sedimentation velocity (data not shown). MAb N8-82 precipitated only a trace amount of the NA, while MAb N8-4 did not precipitate any NA after TM treatment.

These results indicate that NA molecules cannot achieve proper tetramerization in the absence of carbohydrates. Whether or not these oligomers without carbohydrate chains can be transported to the cell surface remains to be determined.

Tetramerization of the NA occurs in the ER of host cells. To identify the cellular compartment in which the NA attains its quartertiary structure, we treated the virus-infected cells with BFA, a fungal metabolite that disrupts the Golgi complex and blocks transport from the ER to the Golgi apparatus (18, 19). Although BFA did not block tetramerization of the NA, as shown by its immunoprecipitation by MAb N8-4 (Fig. 5), the high-molecular-mass species of the NA oligomer was not observed, indicating incomplete processing of oligosaccharides.

The protein transport inhibitor CCCP depletes intracellular ATP, resulting in a blockade of protein export from the ER (2, 3, 12, 23). Treatment with this compound failed to block the appearance of MAb N8-4-reactive forms of the NA, but prevented appearance of the NA oligomer with slower mobility (Fig. 5). That CCCP blocked export to the Golgi apparatus was confirmed by experiments showing inhibition of the acquisition of Endo H resistance (data not presented). The finding that NA precipitated by MAb N8-4 after CCCP treatment was

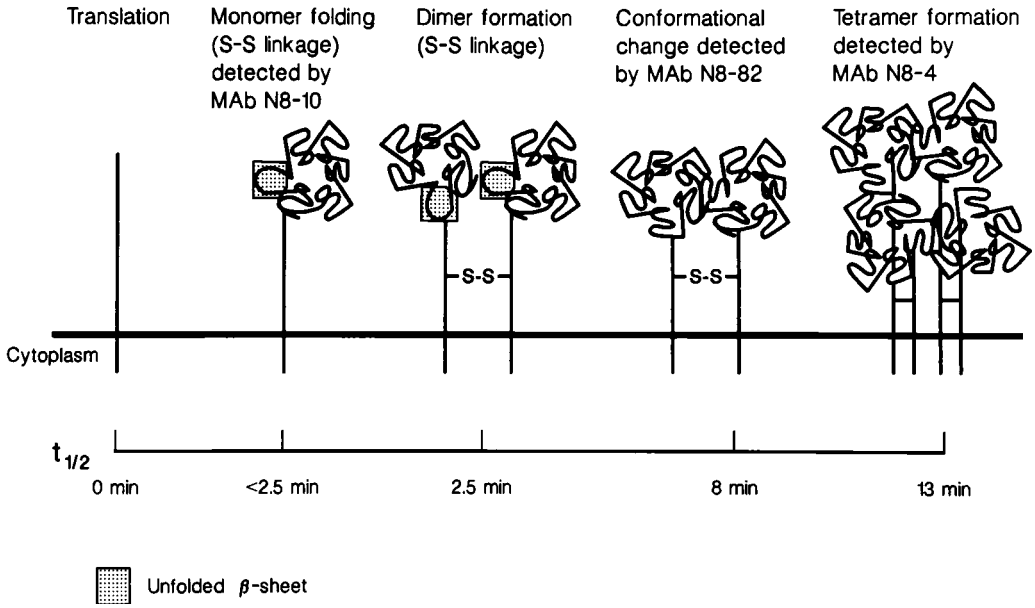

FIG. 8. Proposed steps in the maturation of influenza virus NA. Whether or not the epitope recognized by MAb N8-82 appears on dimeric NA is yet to be determined.

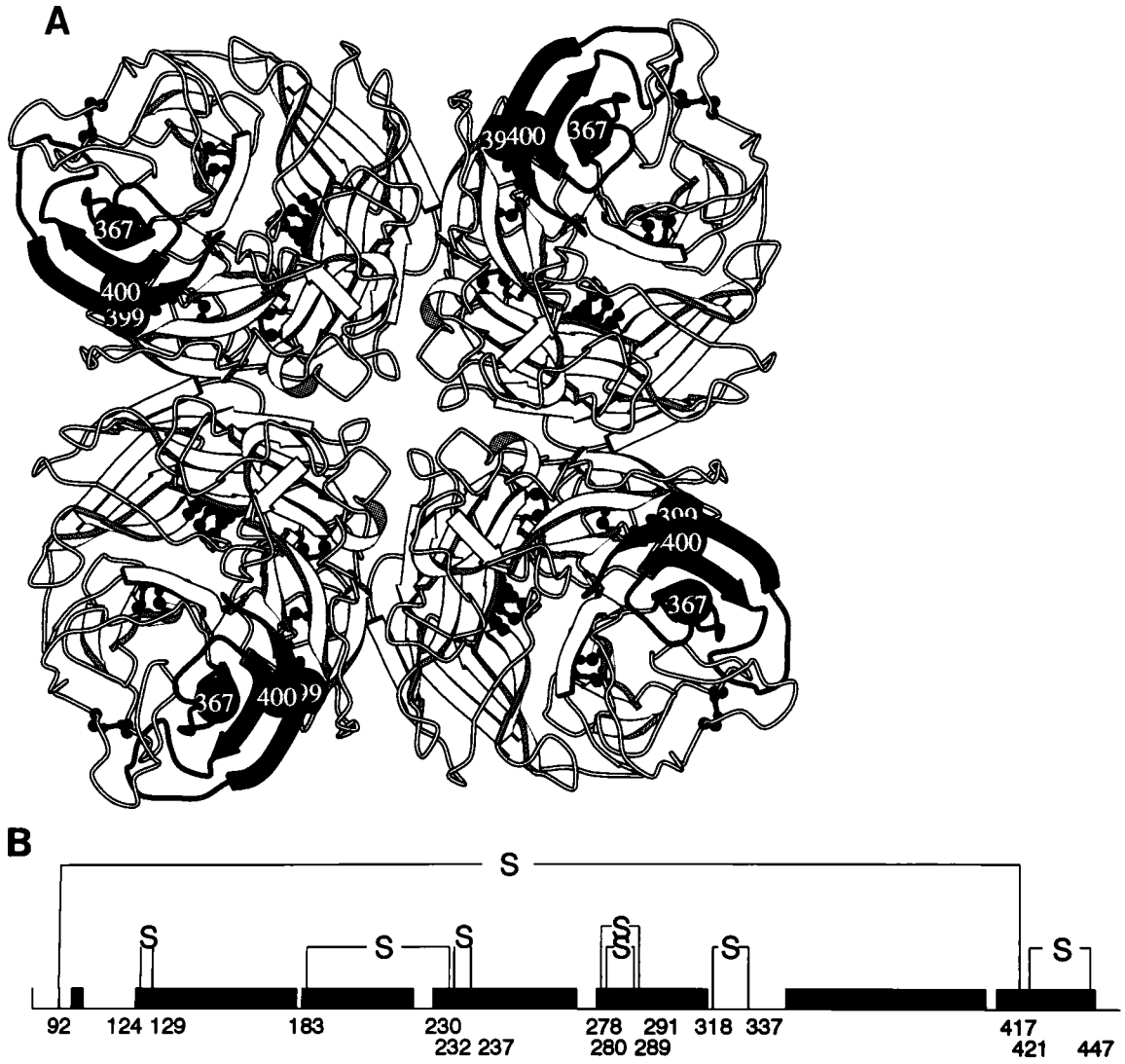

FIG. 9. (A) Three-dimensional structure of N8 NA as written by the MOLSCRIPT program (17). The NA tetramer is viewed from the top, and the β-sheet involving amino acid residues 367, 399, and 400, recognized by MAb N8-82, is highlighted with a bold line. (B) Linear diagram of the N8 NA head (disulfide linkages are shown as S). Numbers at the bottom indicate the positions of cysteine residues. Each of the β-sheets is represented by a solid line. Residues involved in each β-sheet are: β1, amino acids (a.a.) 122 to 176; β2, a.a. 180 to 216; β3, a.a. 224 to 267; β4, a.a. 276 to 316; β5, a.a. 353 to 403; and β6, a.a. 96 to 102 and 407 to 418.

tetrameric was confirmed by sucrose gradient fractionation followed by radioimmunoprecipitation (Fig. 6). These findings indicate that tetramerization of the NA can occur in the ER of virus-infected cells, the site of oligomerization of most, if not all, viral glycoproteins (see reference 11 for a review). This interpretation agrees with the study of Hogue and Nayak (16), demonstrating that the NA tetramer was formed before the acquisition of Endo H resistance.

Temperature sensitivity of the NA assembly. Low temperature (15°C) induces protein accumulation in pre-Golgi vacuoles (22, 23), blocking the transport of glycoproteins to the Golgi apparatus. We therefore conducted chase experiments at 15°C to test the effect of this lower temperature on tetramerization of the NA, which occurs in the ER of host cells. Unexpectedly, chase at 15°C for 45 min (Fig. 7) and 2 h (data not shown) prevented the appearance of the NA tetramer recognized by MAb N8-4. Since the experiments with CCCP and BFA demonstrated that the NA can tetramerize in the ER, the lack of tetramer detection by MAb N8-4 after 15°C incubation seemed irrelevant to protein accumulation in the pre-Golgi vacuoles. Dimerization was also temperature sensitive, as more monomeric NA was detected after chase at 15°C for 45 min than at 37°C (Fig. 7). Finally, at 37°C, 72% of the oligomeric NAs precipitated by MAb N8-10 reacted with MAb N8-82, whereas at 15°C, this fraction was reduced to only 20%.

Temperature sensitivity of oligomerization was observed in influenza A virus HA trimerization (9). Trimerization of the HA occurs more slowly at 15°C than at 37°C ($t_{1/2}$, 110 to 130 min versus 7 to 8 min). Thus, our inability to detect NA tetramers with MAb N8-4 at 15°C probably stems from temperature sensitivity of earlier steps in oligomerization, such as dimerization and/or the conformational change detected by MAb N8-82. Whether or not oligomeric NAs precipitated by MAb N8-82 formed tetramers at 15°C could not be examined, as the amount of radiolabeled oligomer during the 15°C chase was not sufficient for sucrose gradient analysis.

DISCUSSION

Using three MAbs that recognize discrete maturation-associated epitopes on the NA molecule, we were able to identify key events of NA development in virus-infected cells, as depicted in Fig. 8. Folding of the NA monomer probably occurs both during and after translation, as judged by the rapid formation of the epitope recognized by MAb N8-10. Dimerization by intermolecular disulfide linkage was evident soon after subunit folding, with a $t_{1/2}$ of 2.5 min. The epitope recognized by MAb N8-82 appeared on oligomeric NA with a $t_{1/2}$ of 8 min, suggesting a conformational change on the NA subunit. A tetramer-specific epitope recognized by MAb N8-4 appeared with a $t_{1/2}$ of 13 min. Whether or not the putative conformational change detected by MAb N8-82 precedes tetramerization remains to be determined. The site of these processes is the ER of host cells, as demonstrated by experiments with two protein transport inhibitors, BFA and CCCP.

The head domain of the NA consists of six β-sheets and eight pairs of disulfide bonds (Fig. 9) (20), all of which (excluding the one between cysteines 90 and 417) can be regarded as local. These bonds play an important role in folding of the head domain of the NA. Nearly 50% of the radiolabeled NA was already folded and precipitated by MAb N8-10 after 5 min of labeling. Such rapid completion of folding can be attributed to its reliance on local disulfide linkages. Protein disulfide isomerase (PDI) catalyzes the formation and breakage of disulfide bonds in peptides to maintain the correct sets of disulfide linkages (13, 14). Local disulfide linkages may not require PDI to rearrange the linkages to find correct pairs of linkages and therefore may form correct sets of linkages very rapidly.

The β-sheets involving amino acids 367, 399, and 400, recognized by MAb N8-82, is within the longest stretch of amino acids without a disulfide bond (Fig. 9). We propose that the inability of MAb N8-82 to detect monomeric NA might lie in the conformational change of the NA subunit during NA maturation. Because this β-sheet lacks a disulfide linkage, it may not be folded into the same conformation as seen in the mature tetramer during the initial folding process, governed by PDI. After dimerization, the β-sheet may undergo conformational change, resulting in the epitope formation detected by MAb N8-82. If correct, this hypothesis might explain why only the tetrameric form of the NA possesses enzyme activity (6), even though each monomer has an enzyme active site (8). That is, the active site of intracellular monomeric NA may lack a functionally active conformation.

Oligomerization of immature subunits should not be considered unusual, as it has been reported for the HN protein of human parainfluenza virus type 3 (7) and immunoglobulin polypeptide (4). The HN oligomerizes into homo-oligomers, resulting in the absence of detectable monomeric forms of the protein within cells. With the immunoglobulin G heterodimer, completely folded heavy chains are assembled covalently to nascent heavy chains. Moreover, a mutant influenza A virus HA with an incorrectly folded globular head could form trimers (15).

We demonstrated the ER as the site of NA tetramerization in experiments with BFA and CCCP. In addition to blocking the transport of molecules to the Golgi apparatus, BFA causes retrograde transport of Golgi residential proteins into the ER (19). We therefore considered that such proteins may have been responsible for NA tetramerization in the ER during BFA treatment (19). Involvement of the intermediate compartment, which remains intact after BFA treatment (19), also could not be ruled out in experiments with this protein transport blocker. Both possibilities were rejected when the tetramer was detected after treatment with CCCP, which blocks ATP-dependent transport, and hence export from the ER and other distal steps in the transport pathway (2, 3, 12). The formation of the intermediate compartment is considered to be the first ATP-dependent step of export from the ER that is inhibited by CCCP (3).

In summary, we have outlined the steps involved in maturation of the influenza virus NA, using MAbs with different conformational specificities. The possibility of conformational changes in the NA during oligomer maturation is raised by the results with MAb N8-82. Our findings also provide a molecular explanation for the absence of enzymatic function by NA monomers.

ACKNOWLEDGMENTS

We thank Yoshihiro Kawaoka for helpful suggestions, John Gilbert for scientific editing, and Dayna Anderson for typing the manuscript.

This work was supported by Public Health Service research grant AI-08831 from the National Institute of Allergy and Infectious Diseases, Cancer Center Support (CORE) grant CA-21765, and the American Lebanese-Syrian Associated Charities (ALSAC).

REFERENCES

1. **Air, G., and W. G. Laver.** 1989. The neuraminidase of influenza virus. Proteins Struct. Function Genet. **6:**341–356.
2. **Balch, W. E., and D. S. Keller.** 1986. ATP-coupled transport of vesicular stomatitis virus G protein: functional boundaries of secretory compartment. J. Biol. Chem. **261:**14690–14696.
3. **Balch, W. E., M. M. Elliott, and D. S. Keller.** 1986. ATP-coupled transport of vesicular stomatitis virus C protein between the endoplasmic reticulum and the Golgi. J. Biol. Chem. **261:**14681–14689.
4. **Bergman, L. W., and W. M. Kuehl.** 1979. Formation of intermolecular disulfide bonds on nascent immunoglobulin polypeptides. J. Biol. Chem. **254:**5690–5694.
5. **Braakman, L. W., J. Helenius, and A. Helenius.** 1992. Manipulating disulfide bond formation and protein folding in the endoplasmic reticulum. EMBO J. **11:**1717–1722.
6. **Bucher, D. J., and E. D. Kilbourne.** 1972. A_2 (N2) neuraminidase of the X-7 influenza virus recombinant: determination of molecular size and subunit composition of the active site. J. Virol. **10:**60–66.
7. **Colins, P. L., and G. Mottet.** 1991. Homooligomerization of the hemagglutinin-neuraminidase glycoprotein of human parainfluenza virus type 3 occurs before the acquisition of correct intramolecular disulfide bonds and mature immunoreactivity. J. Virol. **65:**2362–2371.
8. **Colman, P. M., J. N. Varghese, and W. G. Laver.** 1983. Structure of the catalytic and antigenic sites in influenza virus neuraminidase. Nature (London) **303:**41–44.
9. **Copeland, C. S., K.-P. Zimmer, K. R. Wagner, G. A. Healy, I. Mellman, and A. Helenius.** 1988. Folding, trimerization, and transport are sequential events in the biogenesis of influenza virus hemagglutinin. Cell **53:**197–209.
10. **Doms, R. W.** 1990. Oligomerization and protein transport. Methods Enzymol. **19:**841–854.
11. **Doms, R. W., R. A. Lamb, J. K. Rose, and A. Helenius.** 1993. Folding and assembly of viral membrane proteins. Virology **193:**545–562.
12. **Doms, R. W., D. S. Keller, A. Helenius, and W. E. Balch.** 1987. Role for adenosine triphosphate in regulating the assembly and transport of vesicular stomatitis virus G protein trimers. J. Cell. Biol. **105:**1957–1969.
13. **Freedman, R. B.** 1984. Native disulfide bond formation in protein biosynthesis: evidence for the role of protein disulfide isomerase. Trends Biochem. Sci. **9:**438–441.
14. **Freedman, R. B.** 1989. Protein disulfide isomerase: multiple roles in the modification of nascent secretory proteins. Cell **57:**1069–1072.
15. **Gething, M.-J., K. McCammon, and J. Sambrook.** 1986. Expression of wild-type and mutant forms of influenza hemagglutinin: the role of folding in intracellular transport. Cell **46:**939–950.
16. **Hogue, B. G., and D. P. Nayak.** 1992. Synthesis and processing of the influenza virus neuraminidase, a type II transmembrane glycoprotein. Virology **188:**510–517.
17. **Kraulis, P. J.** 1991. MOLSCRIPT: a program to produce both detail and schematic plots of protein structures. J. Appl. Crystallogr. **24:**946–950.
18. **Lippincott-Schwartz, J., J. G. Donaldson, A. Schweizer, E. G. Berger, H.-P. Hauri, L. C. Yuan, and R. D. Klausner.** 1990. Microtubule-dependent retrograde transport of proteins into the ER in the presence of brefeldin A suggests an ER recycling. Cell **60:**821–836.
19. **Lippincott-Schwartz, J., L. C. Yuan, J. S. Bonifacino, and R. D. Klauser.** 1989. Rapid distribution of Golgi proteins into the ER in cells treated with

brefeldin A: evidence for membrane cycling from Golgi to ER. Cell **56:**801–813.
20. **Saito, T., Y. Kawaoka, and R. G. Webster.** 1993. Phylogenetic analysis of the N8 neuraminidase gene of influenza A viruses. Virology **193:**868–876.
21. **Saito, T., G. Taylor, W. G. Laver, Y. Kawaoka, and R. G. Webster.** 1994. Antigenicity of the N8 influenza A virus neuraminidase: existence of an epitope at the subunit interface of the neuraminidase. J. Virol. **68:**1790–1796.
22. **Saraste, J., G. Palade, and M. G. Farquhar.** 1986. Temperature-sensitive steps in the transport of secretory proteins through the Golgi complex in exocrine pancreatic cells. Proc. Natl. Acad. Sci. USA **83:**6425–6429.
23. **Tartakoff, A. M.** 1986. Temperature and energy dependence of secretory protein transport in the exocrine pancreas. EMBO J. **5:**1477–1482.
24. **Tatu, U., I. Braakman, and A. Helenius.** 1993. Membrane glycoprotein folding, oligomerization and intracellular transport: effects of dithiothreitol in living cells. EMBO J. **12:**2151–2157.
25. **Taylor, G., E. Garman, R. Webster, T. Saito, and G. Laver.** 1993. Crystallization and preliminary X-ray studies of influenza A virus neuraminidase of subtype N5, N6, N8, and N9. J. Mol. Biol. **230:**345–348.
26. **Yewdell, J. W., A. Yellen, and T. Bachi.** 1988. Monoclonal antibodies localize events in the folding, assembly, and intracellular transport of the influenza virus hemagglutinin glycoprotein. Cell **52:**843–852.